CityZen

megaCITY - Zoom for the Environment

Collaborative Project

7th Framework Programme for Research and Technological Development

Cooperation, Theme 6:

Environment (including Climate Change)

Grant Agreement No.: 212095

Deliverable D2.4.3, type R

Report on reductions of the uncertainties in estimates for direct aerosol forcing and heating by black carbon

Due date of deliverable: project month 24

Actual submission date: project month 36

Start date of project: 1 September 2008 Duration: 36 months

Name of lead beneficiary for this deliverable: PKU

Scientist(s) responsible for this deliverable: Yuanhang Zhang

Contributing authors: Yafang Cheng, Min Hu, Yuanhang Zhang

Project co-funded by the European Commission within the Seventh Framework Programme (2007-2013)		
Dissemination Level		
PU	Public	X
PP	Restricted to other programme participants (including the Commission Services)	
RE	Restricted to a group specified by the consortium (including the Commission Services)	
CO	Confidential, only for members of the consortium (including the Commission Services)	

Report on reductions of uncertainties in estimates of direct aerosol forcing and heating by black carbon

Yafang Cheng, Min Hu, Yuanhang Zhang (yhzhang@pku.edu.cn)

College of Environmental Sciences and Engineering, Peking University, Beijing, China

Tropospheric aerosols affect Earth's climate by altering the radiative properties of the atmosphere through the direct effect of scattering and absorbing sunlight and the indirect effect by changing the properties of clouds [*IPCC*, 2007]. The direct climate forcing of aerosols is difficult to precisely quantify because of the strong dependence of aerosol optical properties on the ambient conditions and other physic-chemical properties [*Seinfeld and Pandis*, 1998] [*Quinn and Coffmann*, 1998] [*Bond et al.*, 1998].

One key parameter governing the aerosol optical properties (AOPs) is its dependence on the ambient relative humidity (RH), which governs the AOPs and depends on the aerosol hygroscopicity [*Covert et al.*, 1972] [*Charlson et al.*, 1992]. The other important parameter is the mixing state of black carbon (BC) (or elemental carbon, EC, or soot). BC is primarily considered as the primary component in aerosol phase strongly absorbing light [*Hansen et al.*, 1979] [*Japar et al.*, 1986] [*Horvath*, 1993] [*Liousse et al.*, 1993] [*Fuller et al.*, 1999] and hence contributes a positive radiative forcing to the climate system [*Hansen et al.*, 1997] [*Jacobson*, 2001]. However, this positive contribution poses one of the largest uncertainties in the estimation of the climate change, e.g., [*Anderson et al.*, 2003], due to deficient knowledge in the mixing state of BC [*Jacobson*, 2001]. To reduce the propagated uncertainties in estimates of direct aerosol forcing, we combined measurement and modeling approaches to determine/derive the two properties and their impact on the radiative forcing.

Another important issue in climate effects of black carbon aerosol is its semi-direct radiative forcing, which is especially important for the strong BC source region, such as mega-city cluster. Cooling of the lower parts of an atmospheric layer, combined with heating aloft and horizontal flux divergence, leads to increased stability of the layer, reduced vertical air exchange, and (assuming constant aerosol sources at the ground) steady increase of particulate pollution in the layer. This enhancement of particle concentrations in turn leads to further warming aloft (due to the absorption of solar radiation by the anthropogenic aerosol particles, soot for example), even stronger stability and further delimited vertical mixing in the layer. Thus, a positive feedback is established in which the presence of the pollutant (absorbing particles) enhances its concentration. Such feedback mechanisms have been detected over South Asia and the Indian Ocean [*Podgorny et al.*, 2000] [*Rama-*

nathan et al., 2001] [*Menon et al.*, 2002] [*Ramanathan and Carmichael*, 2008] and elsewhere [*Jacobson*, 2001]. Suppression of precipitation due to such processes has been hypothesized by [*Zhao et al.*, 2006]. Further studies have discussed about atmospheric stability [*Ramanathan et al.*, 2005] caused by absorption due to aerosol particles. [*Rudich*, 2003] report on increased convection out of the boundary layer into the overlying air induced by aerosol absorption of solar energy. Further effects on regional circulation have been reported by [*Chung and Seinfeld*, 2002] and on evaporation of boundary layer clouds by [*Ackerman et al.*, 2000]. Enhanced stability due to aerosols has also been hypothesized to reduce wind speeds [*Jacobson and Kaufman*, 2006]. However, solid experimental validation of these simulation results is still lacking.

In PRD region, we conducted two international intensive field campaigns, namely PRRID-PRD 2004 and PRID-PRED 2006 [*Zhang et al.*, 2008]. One of the most important tasks designed for these field experiments is to reduce the uncertainties in estimates of direct aerosol forcing and heating by black carbon. Here the major findings regarding the soot mixing state and particle hygroscopicity, as well their related radiative effects, are summarized.

Soot mixing state

The aerosol mixing state was investigated with an optical closure study at Xinken, Pearl River Delta of China [*Cheng et al.*, 2006]. As shown in Figure 1,on the basis of in situ aerosol microphysical and chemical measurements and a two-component aerosol optical model an internal consistency algorithm was developed to model the mass ratio (***r***) of externally mixed black carbon (EC) to total EC, which minimized the discrepancies between measured and calculated optical properties. The rest of EC was assumed to be internally mixed.

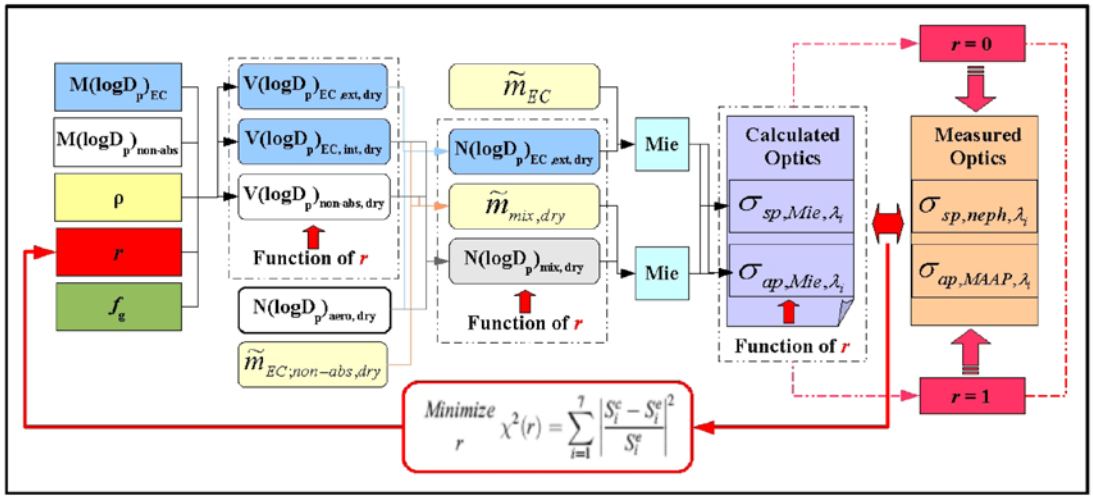

Figure 1. Framework of the dry optical closure and retrieval algorithm of EC mixing state. The explanations of the symbols and functions can be found in the main text.

A time series of r was retrieved. Good agreement between model and observation was found, on the order of ±15% for total/back scattering coefficients and ±10% for absorption coefficient (see Figure 2).

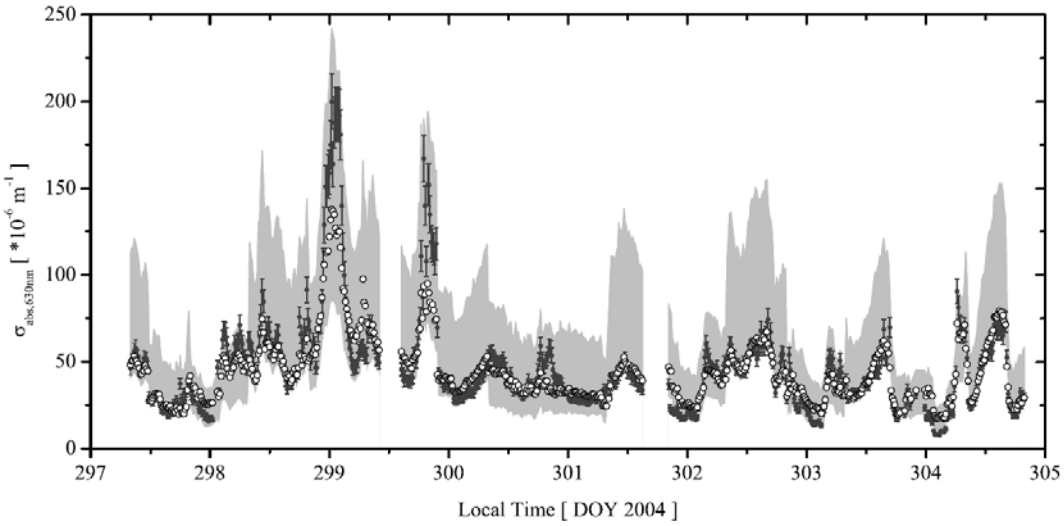

Figure 2. Time series of measured and modeled, absorption coefficient, $\sigma_{abs,MAAP}$ and $\sigma_{abs,Mie}$ at 630 nm. Measurements are represented by black solid points, with error bars indicating double standard deviations (2*s*). The results of the Mie calculation are bounded by the upper and lower limits of the grey area, where the upper/lower limit corresponds to 2*s*.

The retrieved EC mixing state was presented in Figure 3. Strongly dependent of EC mixing state on the local wind patterns at Xinken was found. When north/northeasterly winds prevailed, the air came from the urban and industrial areas of mainland China, and EC was mainly externally mixed with an average r of 85 ± 12%.When the airflow was controlled by a weak local wind system, the mixing state showed a pronounced diurnal variation. During daytime the wind speed was nearly zero. This favored the increase of local pollution, and the average r was about 95%. However, during nighttime the EC mixing state transformed to be internally mixed apparently with an average r of 53 ± 15%, which can be explained by a more aged air mass. The south/southeasterly winds coming from the sea were found to have the most important effect on the transformation of EC mixing state in the night, but fairly rapid local aging processing was also observed.

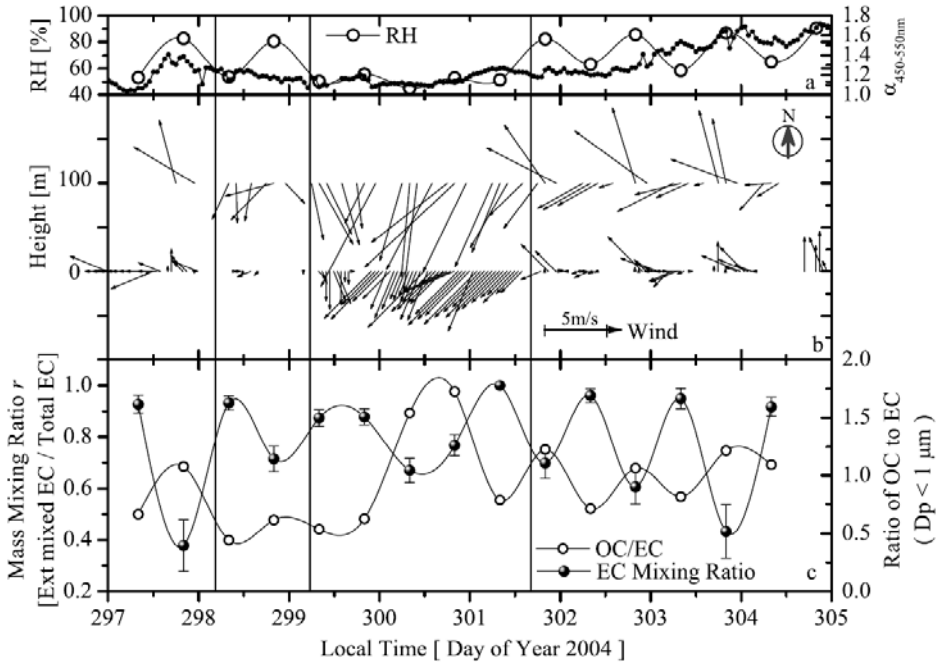

Figure 3.Time series (12-hour) of the mass ratio of externally mixed EC to total EC, with one standard deviation of the retrieval from Monte Carlo simulation as the error bars. Wind patterns are presented as vectors at two vertical heights (ground level and 100 m), as well as 12-hour averaged ambient relative humidities and 1-hour averaged Angström exponent of 450–550 nm.

Hygroscopic growth

Taking the measured particle hygroscopicity into account in the optical (MIE) simulation, as shown in Figure 4, the simulated and observed aerosol extinction at ambient conditions (relative humidities) generally agree with R2 of 0.80 and discrepancy within 10%, except for an outlier on 298.96 DOY. The uncertainties of the two data sets have been taken into account in the linear regression by using the statistical method described in [Brauers and Finlayson-Pitts, 1997], and the results are statistically significant. It should be emphasized that the POLLY lidar observed aerosol extinctions ($\sigma^{amb}_{ep,532nm,POLLY}$) were observed at 60 or 150 – 300m height during night- or daytime, respectively, whereas the modeled values ($\sigma^{amb}_{ep,532nm,Mie}$) are based on the surface measurements. Consequently, good agreement can only be expected during times at which a well-mixed boundary layer was observed (297.5 – 297.79 and 298.5 – 298.79 DOY, [*Tesche*, 2006]). Maximum deviations are observed during 298.96 – 299.04 DOY when a high concentration of pollutants accumulated at the ground due to calm wind during the whole night ([*Cheng et al.*, 2008] [*Eichler*, 2006]).

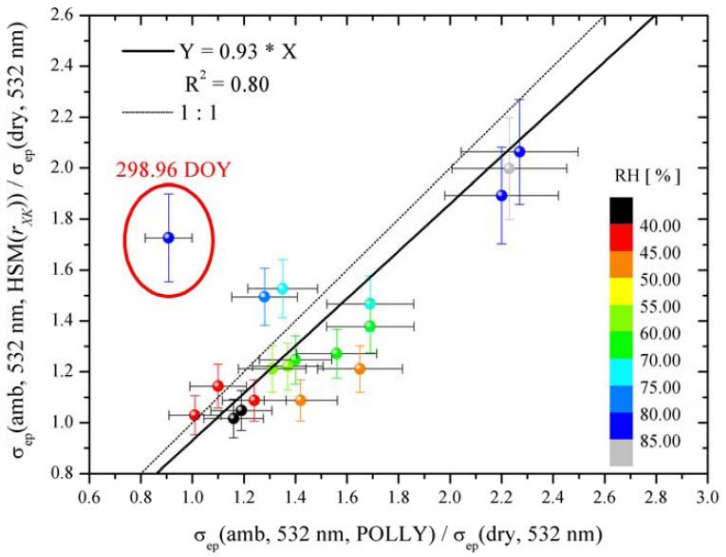

Figure 4.Comparison of the simulated ambient extinction coefficients ($\sigma^{amb}_{ep,532nm,Mie}$) and the one ($\sigma^{amb}_{ep,532nm,POLLY}$) measured at 60m or150–300m during night- and daytime, respectively, by the Raman LIDAR system (POLLY). The ambient extinction coefficients are normalized with those at dry conditions ($\sigma^{dry}_{ep,532nm}$). The error bars are presented as the uncertainties with one standard deviation (*s*, at 68% confidence level), for which only the uncertainties of the simulated and measured $\sigma^{amb}_{ep,532nm}$ have been taken into account, but not the uncertainties of the dry ones.

Influences of relative humidity (RH) on aerosol optical properties and direct radiative forcing are investigated based on observation and modeling studies in the Pearl River Delta region of China. As shown in Figure5a, at 550 nm, the scattering coefficient increases with a factor of 1.54 and 2.31 at a RH increase from 30% to 80% and 90%, respectively. This ratio is mainly controlled by the particle growth factor f_g, and generally increases with increasing wavelength and decreasing particle effective diameter. In 2006, higher hygroscopic growth factors were found in Guangzhou city site due to larger contribution of sea salt [*Liu et al.*, 2008].

Regarding the humidity dependence of single scattering albedo (SSA, ω_0) (see Figure5b), from RH 30% to 90%, the average single scattering albedo (ω_0) changes from ~0.77 to ~0.94. This means along with water coating, absorption and scattering of aerosol particles both increase. As seen in Figure5b, the critical single scattering albedo are not very sensitive to the mixing states and increase with increasing RH ($\omega_{0,crit,550nm}(30\%)$ = 0.77 and $\omega_{0,crit,550nm}(90\%)$= 0.80). The estimated$\omega_{0,crit,550nm}(RH)$ at XK is relatively low compared to the general $\omega_{0,crit,550nm}(RH)$in the polluted areaof 0.85 [*Johnson et al.*, 2004]. By comparing the RH dependence curves of $\omega_{0,crit,550nm}(RH)and\omega_{0,crit,550nm}(RH)$ for different EC mixing states, it is found that if the aerosol at Xinken of PRD is assumed to be externally mixed, the effect of aerosol direct radiative forcing (ΔF_R)in the surface boundary layer is cooling. However, assuming an internal or coated mixing state of EC, no pronouncedΔF_R is observed when RH<60%, i.e., the climate effect of aerosol is at the edge of heating and cooling, whereas a cooling effect can be observed as RH>60%.

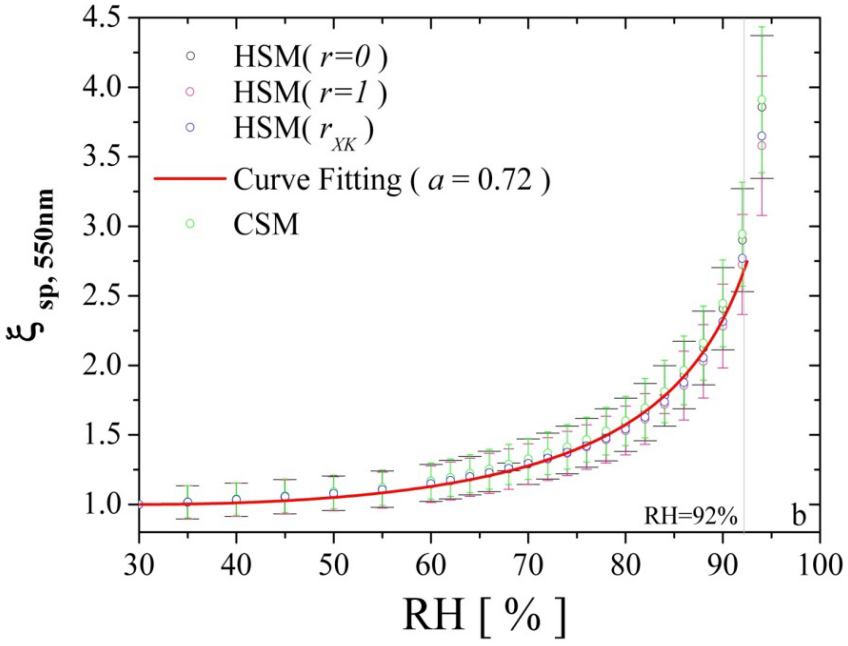

(a)

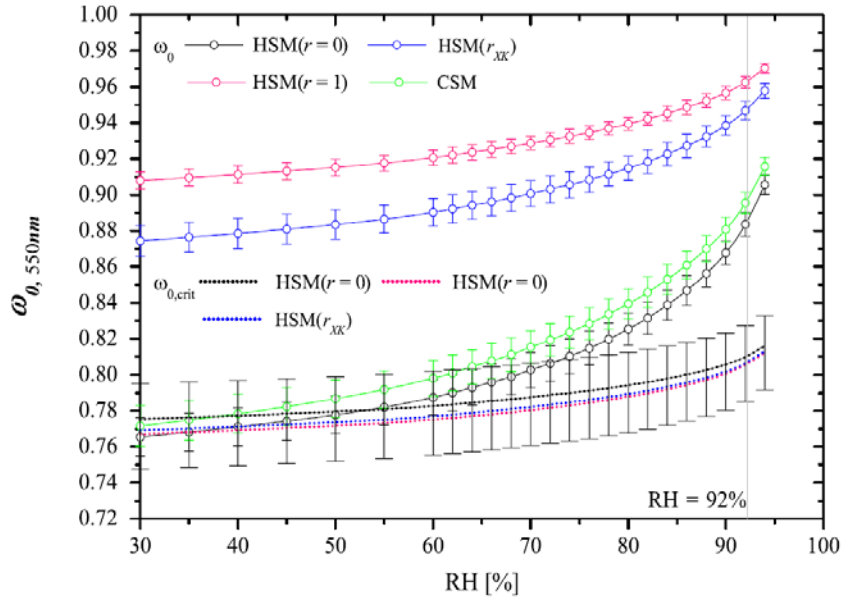

(b)

Figure5.(a) Humidification factors of particle light scattering at wavelength of 550nm. (b) Humidification factors of particle single scattering albedo $\omega_{0,550\ nm}$.

The estimation of aerosol direct radiative forcing (ΔF_R) in the surface boundary layer at XK strongly depends on RH and the EC mixing state, demonstrated in Figure 6. Assuming an internal or coated mixture of EC, no pronounced ΔF_R is observed when RH<60%, whereas a cooling effect arises while RH>60%. Under the actual BC mixing conditions at XK, the effect of ΔF_R is cooling. Over40% of this cooling effect is contributed by water at RH 80% and ΔF_R at RH 90% exceeds that at RH 30% by about a factor of 2.7.

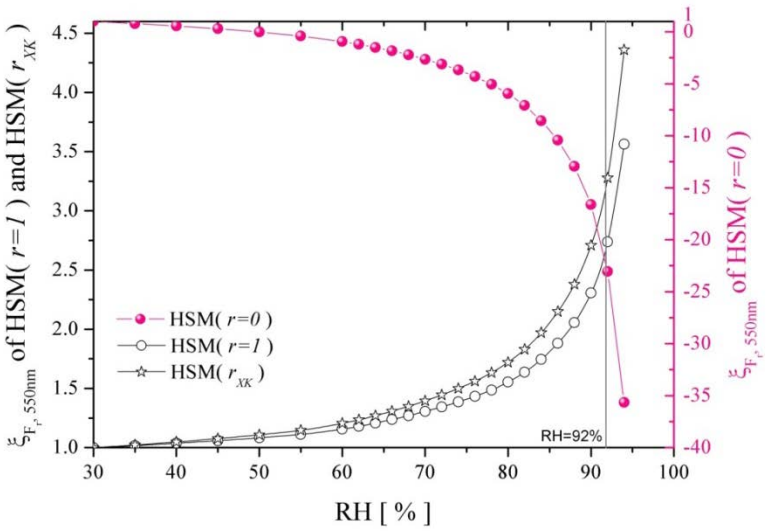

Figure 6. Humidification factor of aerosol direct radiative forcing ($\xi_{FR,550nm}$) in the surface boundary layer of Xinken at wavelength of 550nm for three different mixing states of elemental carbon.

Radiative and dynamic effects of absorbing aerosol particles

Based on the ground measured aerosol hygroscopicity, retrieved EC mixing state and sun-photometer observed aerosol optical depth, a simple radiative transport model [Seinfeld and Pandis, 1998] is used to estimate the aerosol radiative forcing at Xinken, Pearl River Delta of China. The results are presented in Figure 7. It was found that at Xinken, the aerosol radiative forcing is actually very sensitive to the EC mixing state. With increasing wavelength, the "warming" effect is weakened when EC is internally mixed, while the "cooling" effect is strengthened with externally mixed EC or retrieved EC mixing state at Xinken.

The average daytime relative humidity at Xinken during field campaign was about 53%. In general, even with completely internally mixed EC, the "warming" effect is still relatively small with $\Delta F_{R,550nm}$ of $+4\pm2$ Wm^{-2}. However, if EC exists in completely externally mixture, the aerosol "cooling" effects could be as low as -15 ± 4 Wm^{-2}. When taking the actual mixing state of EC at Xinken in to account (r_{XK}), the aerosol radiative forcing is estimated to be about -13 ± 3 Wm^{-2}. This has been far beyond the global average aerosol radiative forcing (-0.3 to -2 Wm^{-2}) and the warming effects of greenhouse gases (+2.5 to +2.7 Wm^{-2}) [*IPCC*, 2007].

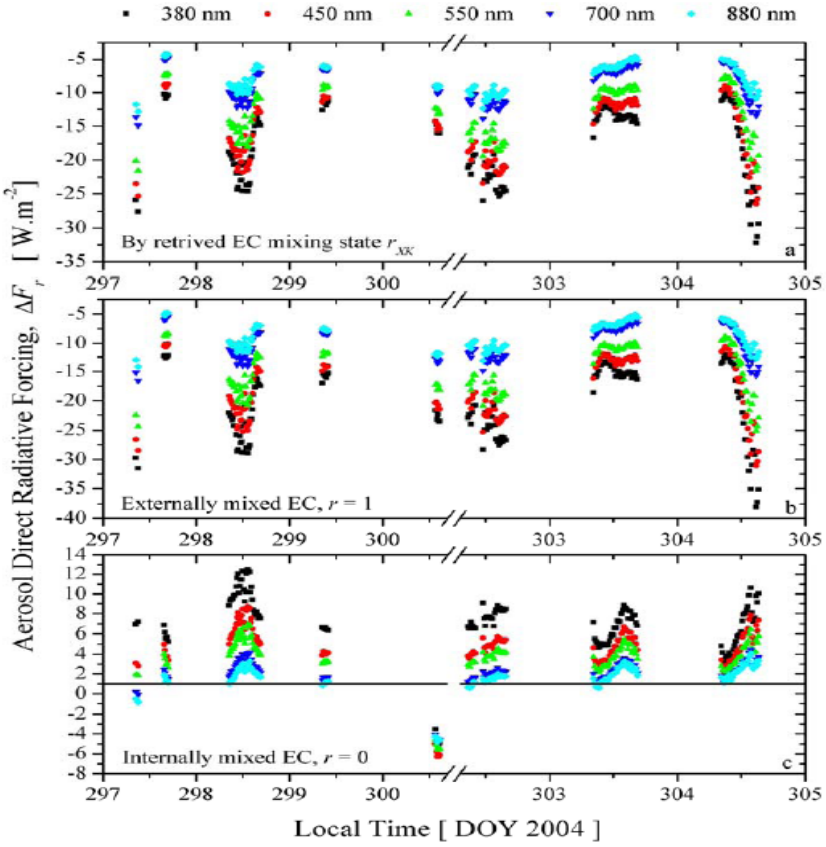

Figure 7.Estimated aerosol direct radiative forcing at 380, 450, 550, 700 and 880nm with three different EC mixing states (internal mixture with r=0, external mixture with r=1 and retrieved EC mixing state r_{XK}).

The radiative and dynamic effects of absorbing aerosol particles were explored based on ground-based measurement campaign conducted in a highly polluted region in southeast of China in October – November 2004 [*Wendisch et al.*, 2008] during the PRDID-PRD campaign [*Zhang et al.*, 2008]. The experiment focused on absorbing aerosol particles and their effects on the solar radiation field and local meteorology. A Raman lidar in conjunction with Sun photometer data measured profiles of particle extinction; ground-based in situ data of aerosol optical properties were collected by nephelometer and absorption photometer. Exceptionally high values of aerosol optical depth of up to 1.5 were observed, with elevated strong absorbing aerosol layers. The radiative simulations were used to drive a dynamic model of the planetary boundary layer (PBL). With this model the temporal course of the height of the PBL was simulated and compared with respective lidar data. The results (see Figure 8) show that the height of the PBL is significantly decreased due to the warming of the aerosol particles at the top of the PBL. In this way, the stabilizing effect of absorbing aerosol particles within the PBL was confirmed by a combination of experimental and modeling means.

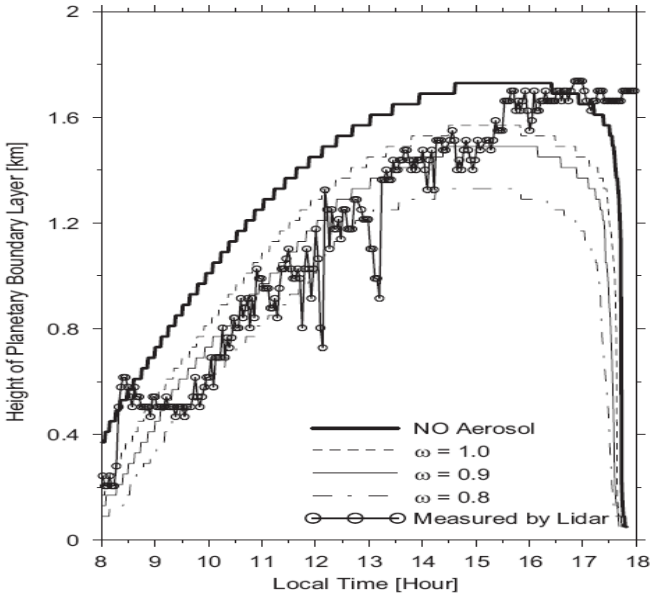

Figure 8. Modeled PBL (planetary boundary layer) heights without aerosol (“NO Aerosol”; thick solid line), and with aerosol and dry particle single-scattering albedos o of 1.0, 0.9 and 0.8. The measured PBL height is marked by a thin solid line with circles.

References

Ackerman, A. S., O. B. Toon, D. E. Stevens, A. J. Heymsfield, V. Ramanathan, and E. J. Welton (2000), Reduction of tropical cloudiness by soot, *Science*, *288*, 1042-1045.

Anderson, T. L., R. J. Charlson, S. E. Schwartz, R. Knutti, O. Boucher, H. Rodhe, and J. Heintzenberg (2003), Climate forcing by aerosols- a Haze picture, *Science*, *300*, 1103-1104.

Bond, T. C., R. J. Charlson, and J. Heintzenberg (1998), Quantifying the emission of light-absorption particles: Measurements tailored to climate studies, *Geophys. Res. Lett.*, *25*(3), 337-340.

Brauers, T., and B. J. Finlayson-Pitts (1997), Analysis of relative rate measurements, *J. Chem. Kinet.*, *29*, 665-672.

Charlson, R. J., S. E. Schwartz, J. M. Hales, R. D. Cess, J. A. C. Jr, J. E. Hansen, and D. J. Hofmann (1992), Climate forcing by anthropogenic aerosols, *Science*, *255*, 423-430.

Cheng, Y. F. et al. (2008), Aerosol optical properties and related chemical apportionment at Xinken in Pearl River Delta of China, *Atmospheric Environment*, *42*(25), 6351-6372, doi:16/j.atmosenv.2008.02.034.

Cheng, Y. F. et al. (2006), Mixing state of elemental carbon and non-light-absorbing aerosol components derived from in situ particle optical properties at Xinken in Pearl River Delta of China, *J. Geophys. Res.*, *111*, 18 PP., doi:200610.1029/2005JD006929.

Chung, S. H., and J. H. Seinfeld (2002), Global distribution and climate forcing of carbonaceous aerosols, *J. Geophys. Res.*, *107*(D19,4407), doi:doi: 10.1029/2001JD001397.

Covert, D. S., R. J. Charlson, and N. C. Ahlquist (1972), A study of the relationship of chemcial composition and humidity to light scattering by aerosols, *J. Appl. Met.*, *11*, 968-976.

Eichler, H. (2006), Hygroscopic behaviour and simulation of the aerosol extinction in Southeast China at ambient conditions, University of Leipzig & Leibniz-Institute for Tropospheric Research (IfT), Leipzig.

Fuller, K. A., W. C. Malm, and S. M. Kreidenweis (1999), Effects of mixing on extinction by carbonaceous particles, *J. Geophys. Res.*, *104*(D13), 15941-15954.

Hansen, J. E., M. Sato, and R. Ruedy (1997), Radiative forcing and climate response, *J. Geophys. Res.*, *102*, 6831-6864.

Hansen, R. H. A. D. A., L. Gundel, and T. Novakov (1979), Identification of the optical absorbing component in urban aerosols, *Appl. Opt.*, *17*, 3859-3861.

Horvath, H. (1993), Atmospheric light absorption - A review, *Atmos. Environ.*, *27A*, 293-317.

IPCC (2007), *Climate Change 2007: The Physical Science Basis. Contribution of Working Group I to the Fourth Assessment Report of the Intergovernmental Panel on Climate Change*, edited by S. Solomon, D. Qin, M. Manning, Z. Chen, M. Marquis, K. B. Averyt, M. Tignor, and H. L. Miller, Cambridge University Press, Cambridge, United Kingdom and New York, NY, USA.

Jacobson, M. Z. (2001), Strong radiative heating due to the mixing state of black carbon in atmospheric aerosol, *Nature*, *409*, 695-697.

Jacobson, M. Z., and Y. J. Kaufman (2006), Wind reduction by aerosol particles, *Geophys. Res. Lett.*, *33*, 6 PP., doi:200610.1029/2006GL027838.

Japar, S. M., W. W. Brachaczek, R. A. Gorse, J. M. Norbeck, and W. R. Pierson (1986), The contribution of elemental carbon to the optical properties of rural atmospheric aerosols, *Atmos. Environ.*, *20*, 1281-1289.

Johnson, B. T., K. P. Shine, and P. M. Forster (2004), The semi-direct aerosol effect: Impact of absorbing aerosols on marine stratocumlus, *Q. J. R. Meteorol. Sci.*, *130*, 1407-1422.

Liousse, C., H. Cachier, and S. G. Jennings (1993), Optical and thermal measurements of black carbon aerosol content

in different environments: Variation of the specific attenuation cross-section, sigma (σ), *Atmos. Environ.*, *27A*(8), 1203-1211.

Liu, X., Y. Cheng, Y. Zhang, J. Jung, N. Sugimoto, S.-Y. Chang, Y. J. Kim, S. Fan, and L. Zeng (2008), Influences of relative humidity and particle chemical composition on aerosol scattering properties during the 2006 PRD campaign, *Atmospheric Environment*, *42*(7), 1525-1536, doi:16/j.atmosenv.2007.10.077.

Menon, S., J. Hansen, L. Nazarenko, and Y. Luo (2002), Climate effects of black carbon aerosols in China and India, *Science*, *297*, 2250-2253.

Podgorny, I. A., W. Conant, V. Ramanathan, and S. K. Satheesh (2000), Aerosol modulation of atmospheric and surface solar heating over the tropical Indian Ocean, *Tellus*, *52B*, 947-958.

Quinn, P. K., and D. J. Coffmann (1998), Local closure during the First Aerosol Characterization Experiment (ACE 1): aerosol mass concentration and scatterring and backscattering coefficients, *J. Geophys. Res.*, *103*(D13), 16575-16596.

Ramanathan, V., and G. Carmichael (2008), Global and regional climate changes due to black carbon, *Nature Geoscience*, *1*, 221-227.

Ramanathan, V., C. Chung, D. Kim, T. Bettge, L. Buja, J. T. Kiehl, W. M. Washington, Q. Fu, D. R. Sikka, and M. Wild (2005), Atmospheric brown clouds: Impacts on South Asian climate and hydrological cycle, *Proceedings of the National Academy of Sciences of the United States of America*, *102*(15), 5326 -5333, doi:10.1073/pnas.0500656102.

Ramanathan, V., P. J. Crutzen, and D. Rossenfeld (2001), Aerosols, climate and the hydrological cycle, *Science*, *294*, 2119-2124.

Rudich, Y. (2003), Influence of the Kuwait oil fires plume (1991) on the microphysical development of clouds, *J. Geophys. Res.*, *108*(D15), doi:10.1029/2003JD003472. [online] Available from: http://europa.agu.org/?uri=/journals/jd/jd0315/2003JD003472/2003JD003472.xml&view=article (Accessed 15 July 2011)

Seinfeld, J., and S. Pandis (1998), *Atmospheric chemistry and physics*, John Wiley & Sons, Inc., New York.

Tesche, M. (2006), Optische und mikrophysikalische Charakterisierung anthropogener Partikel in Sudshina (Pearl River Delta) und Nordchina (Peking) anhand von Ramanlidar- und Sonnenphotometermeassungen, University of Leipzig,.

Wendisch, M. et al. (2008), Radiative and dynamic effects of absorbing aerosol particles over the Pearl River Delta, China, *Atmospheric Environment*, *42*(25), 6405-6416, doi:16/j.atmosenv.2008.02.033.

Zhang, Y. H., M. Hu, L. J. Zhong, A. Wiedensohler, S. C. Liu, M. O. Andreae, W. Wang, and S. J. Fan (2008), Regional Integrated Experiments on Air Quality over Pearl River Delta 2004 (PRIDE-PRD2004): Overview, *Atmos. Environ.*, doi:doi:10.1016/j.atmosenv.2008.03.025.

Zhao, C., X. Tie, and Y. Lin (2006), A possible positive feedback of reduction of precipitation and increase in aerosols over eastern central China, *Geophys. Res. Lett.*, *33*, 4 PP., doi:200610.1029/2006GL025959.